



## Research Article

# M dwarfs found in the first Byurakan spectral sky survey database. Gaia EDR3 and TESS data. Some preliminary results

K. S. Gigoyan<sup>1</sup>, A. Sarkissian<sup>2</sup>, G. R. Kostandyan<sup>1</sup>, K. K. Gigoyan<sup>1</sup>, M. Meftah<sup>2</sup>, S. Bekki<sup>2</sup>, N. Azatyan<sup>1</sup>, and F. Zamkotsian<sup>3</sup>

<sup>1</sup>NAS RA V. A. Ambartsumian Byurakan Astrophysical Observatory (BAO), Byurakan, 0213, Aragatzotn Province, Armenia, <sup>2</sup>Universite de Versailles Saint-Quentin, CNRS/INSU, LATMOS-IPSL, Versailles, France and <sup>3</sup>Aix Marseille University, CNRS, CNES, LAM, Laboratoire d'Astrophysique de Marseille, Marseille, France

### Abstract

In order to gain more information on the 236 M dwarfs identified in the First Byurakan Survey (FBS) low-resolution (lr) spectroscopic database, Gaia EDR3 high-accuracy astrometric and photometric data and Transiting Exoplanet Survey Satellite (TESS) data are used to characterise these M dwarfs and their possible multiplicity. Among the sample of 236 relatively bright ( $7.3 < K_S < 14.4$ ) M dwarfs, 176 are new discoveries. The Gaia EDR3 G broadband magnitudes are in the range  $11.3 < G < 17.1$ . New distance information based on the EDR3 parallaxes are used to estimate the G-band absolute magnitudes. Nine FBS M dwarfs out of 176 newly discovered lie within 25 pc of the Sun. The FBS 0909-082 is the most distant ( $r = 780$  pc) M dwarf of the analysed sample, with a G-band absolute magnitude  $M(G) = 9.18$ ,  $M = 0.59 M_\odot$ ,  $L = 0.13597 L_\odot$ , and  $T_{\text{eff}} = 3844$  K; it can be classified as M1 - M2 subtype dwarf. The nearest is FBS 0250+167, a M7 subtype dwarf located at 3.83 pc from the Sun with a very high proper motion ( $5.13$  arcsec yr<sup>-1</sup>). The TESS estimated masses lie in the range  $0.095 (\pm 0.02) M_\odot \leq M \leq 0.7 (\pm 0.1) M_\odot$  and  $T_{\text{eff}}$  in the range  $4000 \text{ K} < T_{\text{eff}} < 2790 \text{ K}$ . We analyse colour-colour and colour-absolute magnitude diagram (CaMD) diagrams for the M dwarfs. Results suggest that 27 FBS M dwarfs are double or multiple systems. The observed spectral energy distribution (SED) for some of the M dwarfs can be used to classify potential infrared excess. Using TESS light curves, flares are detected for some FBS M dwarfs. Finally, for early and late sub-classes of the M dwarfs, the detection range for survey is estimated for the first time.

**Keywords:** Surveys: TESS and Gaia data – Stars – stars: late-type

(Received 27 October 2022; revised 4 March 2023; accepted 6 April 2023)

## 1. Introduction

M-dwarf stars are most common stars, representing more than 75% of all stars within our Galaxy (Henry et al. 2006, 2018). They dominate the stellar populations by number, but have a very low mass range  $0.075 M_\odot \div 0.50 M_\odot$  and effective temperature ( $T_{\text{eff}}$ ) less than 4000 K (Delfosse et al. 2000). M dwarfs are main-sequence stars whose spectra display bands of TiO and other molecules such as CaH, CaOH, VO, FeH, and CrH (Kirkpatrick et al. 1993; Johnson et al. 1986). Low luminosity M dwarfs are of interest for both observational and theoretical reasons. The faintest M dwarfs include stars undergoing gravitational collapse to the main-sequence, stars burning hydrogen on the main-sequence, and stars with a mass too low to burn hydrogen, the ‘brown dwarfs’. These stars show frequent flaring, in the Johnson U photometric band up to 6 mag. The spectra of most flaring stars also show strong hydrogen Balmer, calcium H and K, helium, and sodium emission lines.

The great majority of the M dwarfs discoveries has been based on the study of the proper motion catalogues, such as Lowell

Observatory Proper Motion (Giclas, Burnham, & Thomas 1971), the proper motion ‘Catalogue of Nearby Stars, 3rd edition-CNS3’ (Gliese & Jahreiss 1991), and the ‘New Luyten Two Tenths’ (NLTT) catalogue of Luyten (1979–80), which includes 58845 stars with proper motions larger than  $0.18$  arcsec yr<sup>-1</sup>. The presence of numerous M dwarfs has been confirmed among the proper motion objects in the Lépine & Shara (2005) catalogue.

More than two decades later, the discoveries of the high proper motion objects using the SuperCOSMOS Sky Survey are the primary target of the Research Consortium on Nearby Stars (RECONS; Henry et al. 1997), on-line access via <https://www.recons.org> survey. RECONS is currently extending the survey work to 25 parsecs. The RECON program (Jao et al. 2005; Henry et al. 2018) started analysing astrometry data in 1999, targeting red, brown, and white dwarfs within 25 pc.

Studies of M dwarfs two decade ago were limited by the number of available M dwarf spectra (Delfosse et al. 1998, 1999) because of the difficulty of measuring reliable spectra from these faint objects. However, with the development of modern astronomical facilities, the number of M dwarf spectra has been increasing dramatically. West et al. (2011) presented the spectroscopic catalog including 70841 M dwarf spectra from Sloan Digital Sky Survey (SDSS) Data Release 7 (Abazajian et al. 2009), providing fundamental spectroscopic data on M dwarfs for probing Galactic chemical evolution. Recently, Zhong et al. (2019) presented a new catalog of M dwarf and M giant stars from the LAMOST (Large Sky

**Corresponding author:** K. S. Gigoyan, Email: [kgigoyan@bao.sci.am](mailto:kgigoyan@bao.sci.am).

**Cite this article:** Gigoyan KS, Sarkissian A, Kostandyan GR, Gigoyan KK, Meftah M, Bekki S, Azatyan N and Zamkotsian F. (2023) M dwarfs found in the first Byurakan spectral sky survey database. Gaia EDR3 and TESS data. Some preliminary results. *Publications of the Astronomical Society of Australia* 40, e023, 1–15. <https://doi.org/10.1017/pasa.2023.20>

Area Multi-Objects Fiber Spectroscopic Telescope (Cui *et al.* 2012) release 5 (DR5) database. 501152 M dwarfs have already been identified based on a classification algorithm. Spectroscopic confirmations of thousands of M dwarfs identified in proper motion catalogues are also being provided in two big series of the papers, namely ‘The Solar Neighborhood’ (Vrijmoet *et al.* 2022), and in series of the papers ‘Meeting The Cool Neighbors’ (Cruz *et al.* 2018).

M dwarf study has become of central interest for astronomy in the last two decades, notably for their application to exoplanet research (Tarter *et al.* 2007). The small radii, low mass, and low luminosity facilitate the discovery of orbiting low-mass planets via radial velocity (RV) and transiting photometry (Muirhead *et al.* 2012; Martinez *et al.* 2017; Mann *et al.* 2018). Recently, the Calar Alto High-Resolution search for M dwarfs with the Exoearth with Near-infrared and optical Echelle Spectrograph (CARMENES) (Quirrenbach *et al.* 2014, 2018), and HARPS (Astudillo-Defru *et al.* 2017) surveys are targeting planets (extra-solar planets) around M dwarfs (Espinoza *et al.* 2022; Alonso-Floriano *et al.* 2015; Cifuentes *et al.* 2020). CARMENES is a stabilised, high-resolution, double-channel spectrograph at the 3.5 m Calar Alto telescope, which is monitoring M dwarfs to detect exoplanets with the RV method.

The main goal of the present paper is the characterisation of Galactic M dwarfs selected on First Byurakan Survey (FBS) plates (Gigoyan, Mickaelian, & Kostandyan 2019), using modern astronomical databases, mainly *Gaia* EDR3 (Brown *et al.* 2021) and TESS (Transiting Exoplanet Survey Satellite; Stassun *et al.* 2019). This paper presents the preliminary results for FBS M dwarfs and is structured as follows. Section 2 introduces the FBS for late-type stars (LTSs) and its digitised version and characterise our sample of 236 M dwarfs, Section 3 presents spectroscopic observations for selected M dwarfs. Section 4 considers photometric and astrometric data, cross-correlations with *Gaia* EDR3, TESS, GALEX, and ROSAT catalogues, colour-colour and colour-absolute magnitude diagrams (CaMD), and spectral energy distribution of FBS M dwarfs, paying particular attention to the FBS 0250+167 star. Section 5 discusses possible multiplicity and companions around M dwarfs. A TESS light curve analysis for FBS M dwarfs is presented in Section 6. Finally, Section 7 recalls the main results obtained for the FBS M dwarfs and provides concluding remarks.

## 2. Target selection. FBS late-type stars catalog

All M dwarfs analysed here are presented in ‘The Second Revised and Updated Version of the FBS Late-Type Stars (LTSs) Catalogue’ at high Galactic latitudes, which is a comprehensive list of 1471 objects (131 C (carbon) stars, 1104 M giants and 236 M dwarfs, Gigoyan *et al.* (2019), SIMBAD CDS Vizier Catalogue J/MNRAS/489/2030). LTSs are selected on the Digitized First Byurakan Survey (DFBS). Its images and spectra are available on the DFBS web portal in Trieste (I <https://www.ia2-byurakan.oats.inaf.it/>) plates, which is a digitised version of the FBS (Markarian *et al.* 1989). From the 236 identified M dwarfs, 176 are new discoveries and 60 M dwarfs are proper motion objects known mainly from the ‘New Luyten Two-Tenth’-NLTT catalogue (SIMBAD Vizier Catalogue I/98A), and from the Lépine & Shara (LSPM; 2005). For the great majority of the known proper motion objects, Gigoyan *et al.* (2019) reported M dwarf

spectral types. The limiting magnitude on different plates varies in the range 16.5<sup>m</sup>–19.5<sup>m</sup> in V, however, for the majority it is 17.5<sup>m</sup>–18.0<sup>m</sup>. C stars can be identified through the presence of Swan bands of the C<sub>2</sub> molecule and M-type stars can easily be distinguished thanks to the TiO molecule absorption bands (Gigoyan *et al.* 2001).

## 3. Optical spectroscopy

### 3.1. BAO 2.6 m telescope spectra

For FBS LTSs, medium-resolution CCD spectra are obtained at different epochs with the BAO (Byurakan Astrophysical Observatory) 2.6-m telescope (spectrographs UAGS, ByuFOSC2 and SCORPIO). Figure 1 presents examples of optical spectra for three FBS M dwarfs obtained with the SCORPIO spectrograph and an EEV 42-402048 × 2048 pixel CCD.

### 3.2. LAMOST spectra

Moderate-resolution CCD spectra for 44 FBS M dwarfs (out of 236, presented by Gigoyan *et al.* 2019) were secured by LAMOST (Large Sky Area Multi-Object Fiber Spectroscopic Telescope) observations (Luo *et al.* 2019, LAMOST DR7, spectra available on-line at <http://dr7.lamost.org/search/>, also see SIMBAD Vizier Catalog V/156/dr7/lrs). Figure 2 shows the LAMOST moderate-resolution CCD spectra for four FBS M dwarfs.

### 3.3. CAFOS observations

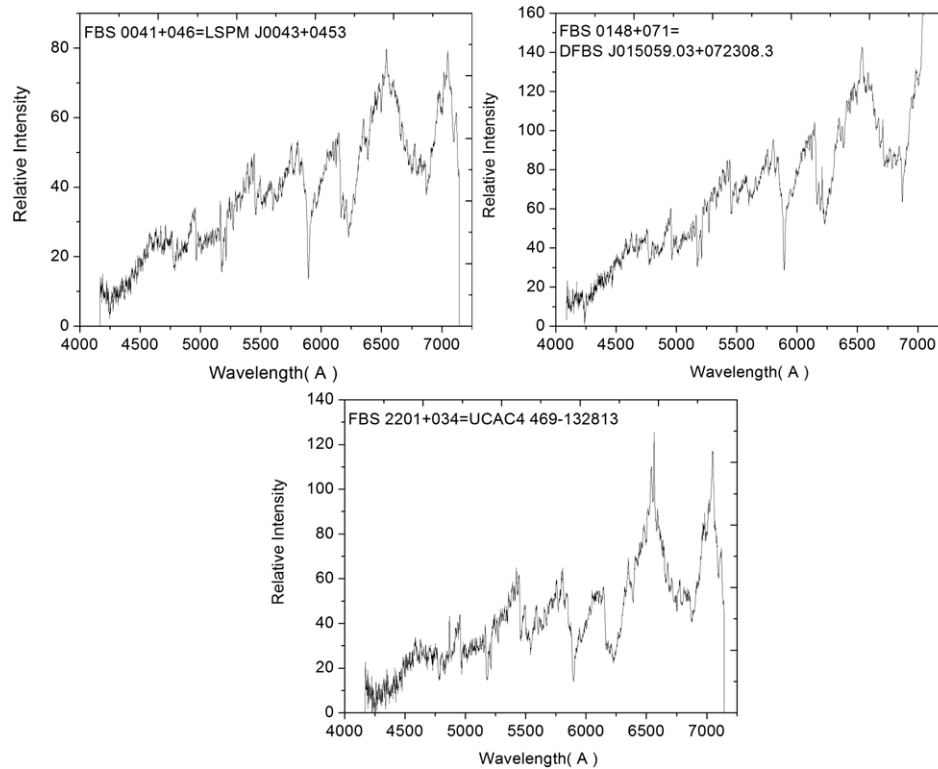
Observations for some amount of FBS M dwarfs were also secured with Calar Alto Focal Reductor and Spectrograph (CAFOS) mounted on the Ritchey-Chretien focus of the Zeiss 2.2 m Calar Alto telescope. Observations were carried out using G-100 grism, which resulted in a useful wavelength range of 4200–8300 Å at a resolution  $R \sim 1500$  (Alonso-Floriano *et al.* 2015). Spectral types are presented by these authors for 753 M dwarfs (SIMBAD Vizier Catalogue J/A+A/577/A128/Mstars/). For an accurate determination of spectral sub-classes, Alonso-Floriano *et al.* also observed standard stars with well-determined spectral types from M0 to M8.

Table 1 lists CAFOS observations of 6 FBS M dwarfs (out of the 12 stars observed), namely FBS number, ‘Karmn’ (number with CARMENCITA identifier following the Karmn nomenclature format (CARMENCITA-CARMENES Cool dwarf Information and data Archive, Alonso-Floriano *et al.* (2015)), associations in SIMBAD database, 2MASS (Two Micron All-Sky Survey, Skrutskie *et al.* 2006) J magnitude, and spectral subclasses estimated (SIMBAD Vizier Catalogue JJ/A+A/577/A128/M stars, ‘CARMENES input catalogue of M dwarfs’).

## 4. Astrometric and photometric data

### 4.1. Gaia EDR3 data

*Gaia* EDR3 (Gaia Collaboration; Brown *et al.* 2021) provides high-precision astrometry, three-band photometry, effective temperatures, and information on astrophysical parameters for about 1.8 billion sources over the full sky brighter than  $G = 21.0$  mag. All FBS M dwarfs were cross-matched with the *Gaia* EDR3 catalogue sources. These objects are relatively bright, so that G-band brightnesses were in the range  $11.3 < G < 17.1$  mag.



**Figure 1.** BAO 2.6-m telescope spectra for three FBS M dwarfs, obtained on 2018 September 8/9 with the SCORPIO spectrograph, using a  $600 \text{ line mm}^{-1}$  grism and CCD EEV 42-40 in spectral range  $\lambda 4000\text{--}7000 \text{ \AA}$  (pixel size  $13.5 \mu\text{m}$ , resolution  $\sim 6 \text{ \AA}$ ).

#### 4.2. TESS observations

NASA's Transiting Exoplanet Survey Satellite (TESS) is an all-sky space-based mission designed to search for planets transiting around nearby M dwarfs (Ricker et al. 2014). Launched in 2018 April, it started regular science operation on 2018 July 25. Its observed  $\sim 73\%$  of the sky across 26 sectors, each lasting 27.4 d and covering a  $24^\circ \times 96^\circ$  field of view. TESS observed a number of stars at 2-min cadence and collected full frame images (FFIs) every 30 min, covering the entire mission phase. By the end of 2 two-year primary mission, TESS identified 2241 exoplanet candidates (Guerrero et al. 2021), known as TESS Objects of Interest (TOIs).

We have cross-correlated our list of 236 M dwarfs with the TESS Input Catalog, Version 8.2 (TIC v8.2, Paegert et al. 2021, SIMBAD CDS VizieR Catalog IV/39/tic82), giving the data for FBS dwarf M stars (Stassun et al. 2018), notably multiple key physical parameters for stars, parallaxes, proper motions, TESS(T) magnitudes, temperatures, masses, and luminosities in solar units.

#### 4.3. GALEX ultraviolet detection

We have cross-correlated the FBS M dwarfs against the GR6+7 data release of the GALEX (Galaxy Evolution Explorer, far-UV band  $\lambda_{\text{eff}} \sim 1528 \text{ \AA}$  (FUV, 1344–1786  $\text{\AA}$ ) and near-UV,  $\lambda_{\text{eff}} \sim 2310 \text{ \AA}$  (NUV, 1771–2831  $\text{\AA}$ ). To match sources in the GALEX data with the FBS M dwarf sample, we searched GALEX (SIMBAD VizieR Catalogue II/335/galex-ais, Bianchi, Shio & Thilker (2017) data to identify UV sources within  $5''$  and found GALEX counterparts for 43 FBS M dwarfs (out of 176 new discoveries) using  $5''$  search radius.

#### 4.4. ROSAT

Our list of all FBS M dwarfs was cross-correlated also with both the ROSAT All-Sky Survey Faint Source Catalog (Voges et al. 2000) and the Second ROSAT All-Sky Survey (2RXS) Source Catalog (Boller et al. 2016). We used a search radius of 15 arc-sec, which is on the order of the astrometric precision of the ROSAT catalog. Our search identified 20 M dwarfs with the X-ray counterparts.

#### 4.5. 2MASS

Giant stars are notable for having infrared colours different from the M dwarfs, most apparent in near-infrared (NIR) a (J-H vs H-K) colour-colour. This has been known since Bessell & Brett (1988) and Bessell (1991). M dwarfs have comparatively blue J-H colours than giants. The 2MASS J-H versus H-K<sub>s</sub> colour-colour plots for all 1471 FBS M- and C-type stars, indicating their luminosity classes are presented in paper by Gigoyan et al. (2019).

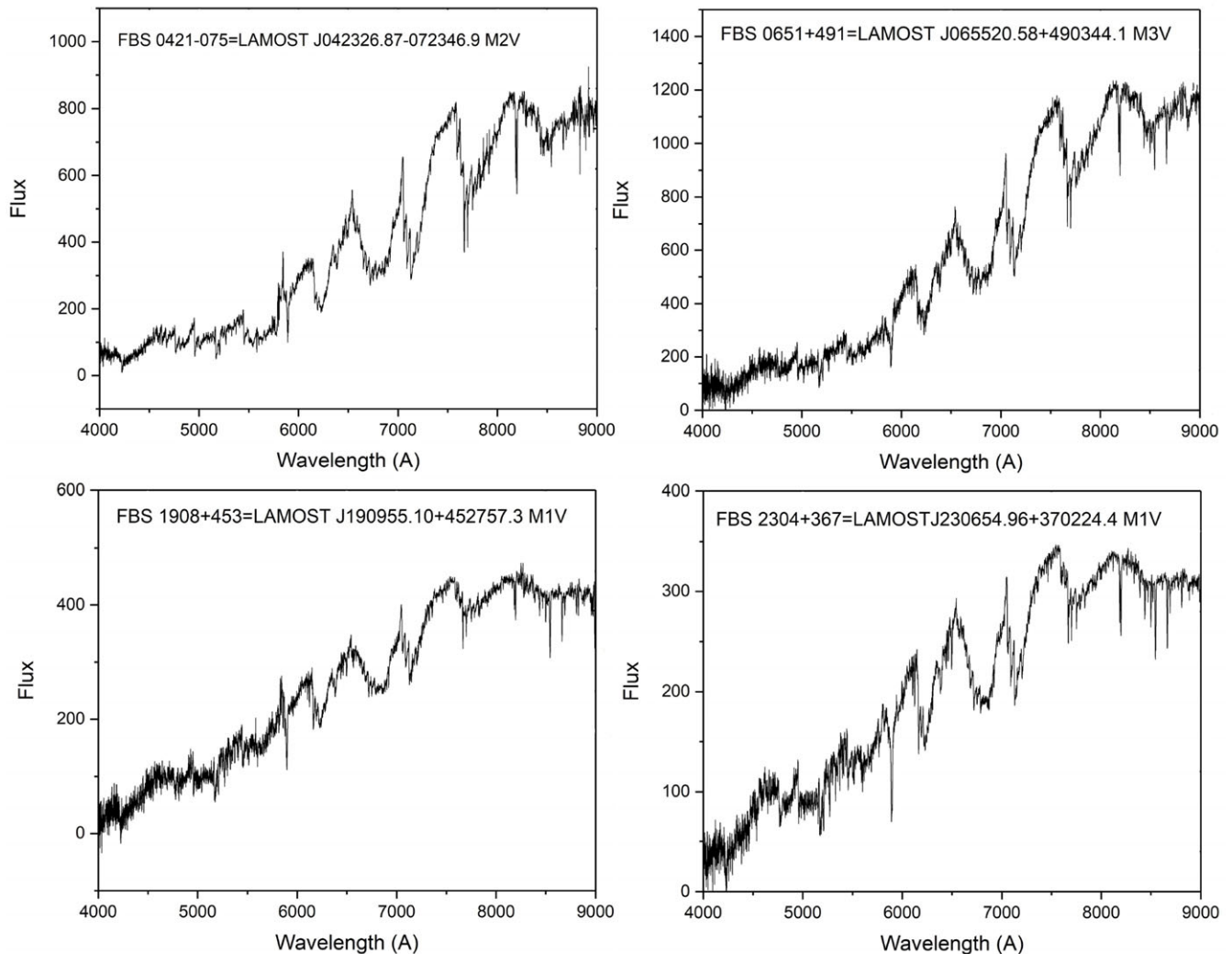
Among all FBS M dwarfs, the FBS 0250+167 star is rather exceptional with its extremely high proper motion (2MASS 02530084+1652532,  $J - H = 0.511$ ,  $H - K_s = 0.298$ ). This object was discovered on the FBS plate No 117 (Kodak—IIAF, obtained on 1-m Schmidt telescope 1969 November 13). In our XIV-th list of the LTSS, we present this object as M7-M8 subtype star (Gigoyan et al. 2003). Figure 3 shows the DSS1 R and DSS2 R finder charts and 1r 2D spectral shape of the FBS 0250+167 star.

Figure 4 presents the direction of the motion of the high proper motion star FBS 0250+167, which was constructed, using DSS1, DSS2, DFBS Plate No117 data and also *Gaia* EDR3 high accurate astrometric data (*Gaia* EDR3 35227046884571776).

**Table 1.** CAFOS spectral types for 6 FBS M dwarfs.

| FBS number | 'Karmn' number | SIMBAD association    | J mag | Sp. type | Date       |
|------------|----------------|-----------------------|-------|----------|------------|
| 0444-113   | J04468-112AB   | 1RXS J044652.0-111658 | 8.14  | M4.9V    | 2013-02-14 |
| 0928+026   | J09308+024     | 1RXS J093051.2+022741 | 9.42  | M4.0V    | 2012-01-04 |
| 1040-089   | J10430-092AB   | WT1827                | 9.67  | M5.5V    | 2012-01-09 |
| 1527+469   | J1529.0+4646   | 1RXS J152902.1+464627 | 9.94  | M4.5V    | 2012-02-09 |
| 1652+631   | J16528+610     | LSPM J1652+6304       | 9.59  | M6.0V    | 2012-08-06 |
| 2201+034   | J22035+036AB   | 1RXS J220330.8+034001 | 9.74  | M4.0V    | 2012-01-04 |

1RXS—'ROSAT Bright Survey', Fisher *et al.* 1998–2000, SIMBAD CDS VizieR Catalog IX/32/notes. LSPM—'A Catalog of Northern Stars with Annual Proper Motions Larger than 0.15 arcsec yr<sup>-1</sup>', Lépine & Shara (2005). WT1827—Alonso-Floriano *et al.* (2015).

**Figure 2.** LAMOST moderate-resolution CCD spectra in the range 4000–9000 Å for a sample of FBS M dwarfs.

Moderate-resolution CCD spectra for object FBS 0250+167 in the wavelength range  $\lambda$ 3940–8500 Å were obtained on 10 of 2007 February with the 1.52 m Cassini telescope of the Bologna (Italy) Astronomical Observatory at Loiano (equipped with the Bologna Faint Object Spectrometer and Camera—BFOSC, 1300 × 1340 pixel EEV P129915 CCD). The spectra are shown in Figure 5, where relative fluxes corrected for atmospheric extinction are plotted on the Y-axis. The correction for the instrumental

response was also applied. The spectra were reduced by means of standard IRAF<sup>a</sup> procedures.

The discovery of this very high proper motion star was reported for the time in 2003 May by Teegarden *et al.* (2003) who called the star SO 025300.5+165258 (object is also known as Teegarden's

<sup>a</sup>IRAF is distributed by the NOAO which is operated by AURA under contract with NFS.

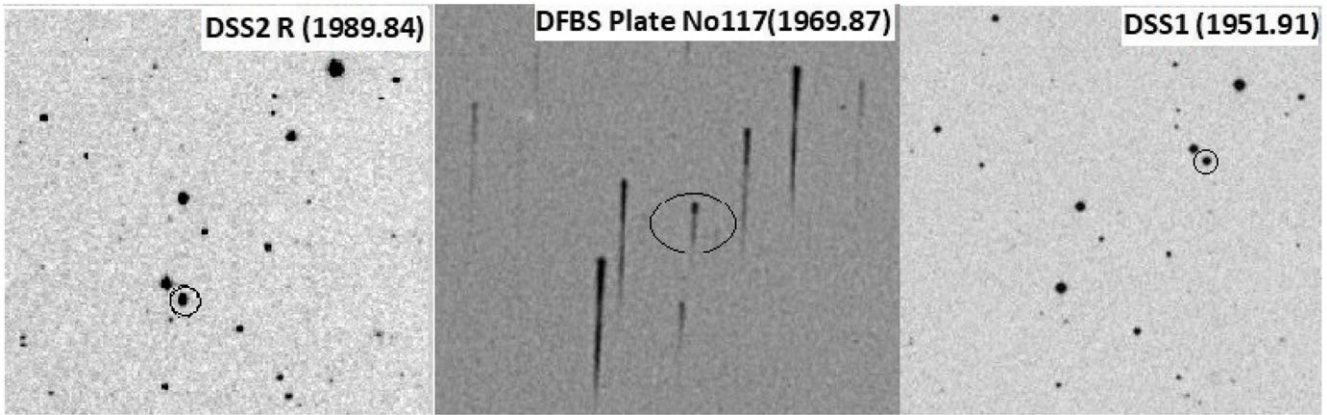


Figure 3. DSS1 R and DSS2 R, finder charts, also DFBS Ir 2D spectral shape on the plate N117 for very high proper motion star FBS 0250+167.

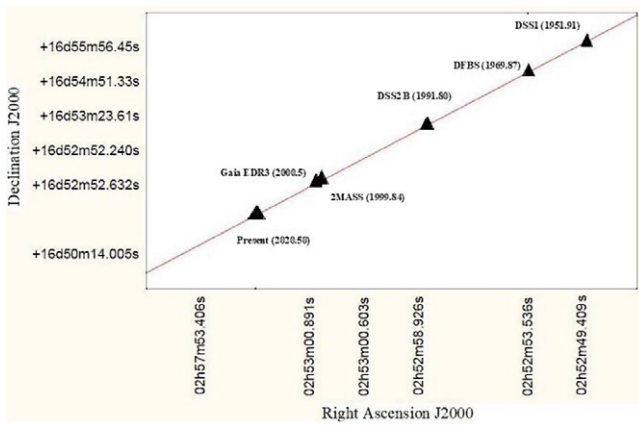


Figure 4. Direction of the motion of the very high proper motion (PM = 5.12 arcsec yr<sup>-1</sup>) star FBS 0250+167 which was found due to DFBS plate N117.

star). Teegarden et al. used the Sky Morph database of the Near Earth Asteroid Traking (NEAT) project (Pravdo et al. 1999). We discuss Teegarden’s star (SO 025300.5+165258=FBS 0250+167) in this context because this star is the brightest and one of the nearest ultracool dwarf in the solar neighbourhood. As part of CARMENES search for exoplanets around M dwarfs, Zechmeister et al. (2019) obtained 245 RV measurements for FBS 0250+167 and analysed them for planetary signals (Figure 3 of paper by Zechmeister et al. 2019, see also for plots SIMBAS VizieR Catalog J/A+A/627A49). Zechmeister et al found periodic variability in the RV indicative of two planet candidates, each with 1.1 M<sub>⊙</sub> minimum mass orbiting at periods of 4.91 and 11.4 d, respectively. These two planets are among the lowest-mass planets discovered so far. This star exhibits occasional flares (Figure 1 of Zechmeister et al. 2019). TIC v8.2 catalogue gives the following data for FBS 0250+167 (TIC Identifier is 257870150, M = 0.095 M<sub>⊙</sub>, L = 0.00077 L<sub>⊙</sub>, T<sub>eff</sub> = 2790 K, and V = 15.13 mag).

4.6. Colour-absolute magnitude (CaMD) diagrams based on Gaia DR3 and TESS data

Figure 6 presents the observational Gaia EDR3 absolute magnitude (M(G)) versus BP-RP colour, or Hertzsprung-Russell Diagram-HRD) for all FBS detected M dwarfs. For comparison,

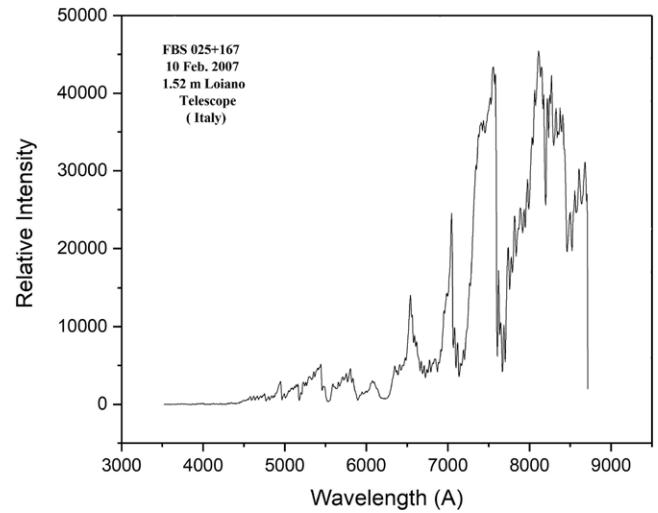


Figure 5. The 1.52 m Bologna telescope spectrum for FBS 0250+167, covering the wavelength range 4000–8500 Å.

the results for FBS M and C giants are also shown on the same diagram (Gigoyan et al. 2019).

We have used the distance information derived from Gaia EDR3 by Bailer-Jones et al. (2021). The absolute G-band magnitude is estimated using the common equation:

$$M(G) = G - 5Logr + 5 - A(G) \tag{1}$$

A(G) is assumed to be very low for our objects because they are at high Galactic latitudes.

Meanwhile, this CaMD needs to be studied in more detail to age date for all FBS M dwarfs using various models (for example, isochrones BHAC15, Baraffe et al. 2015).

The panels (a, b) in Figure 7 show the absolute M(V) magnitude as a function of the optical-to-infrared V-J and V-K colour for FBS M dwarfs (J and K magnitudes are from the 2MASS database based on TESS Input Catalog data (SIMBAD CDS VizieR Catalog IV/39/tic82).

Figure 8 presents the histogram of the Gaia EDR3 G-wide band magnitude distribution of the FBS M dwarfs and M dwarfs which are known proper motion objects, mainly from NLTT and LSPM catalogues.

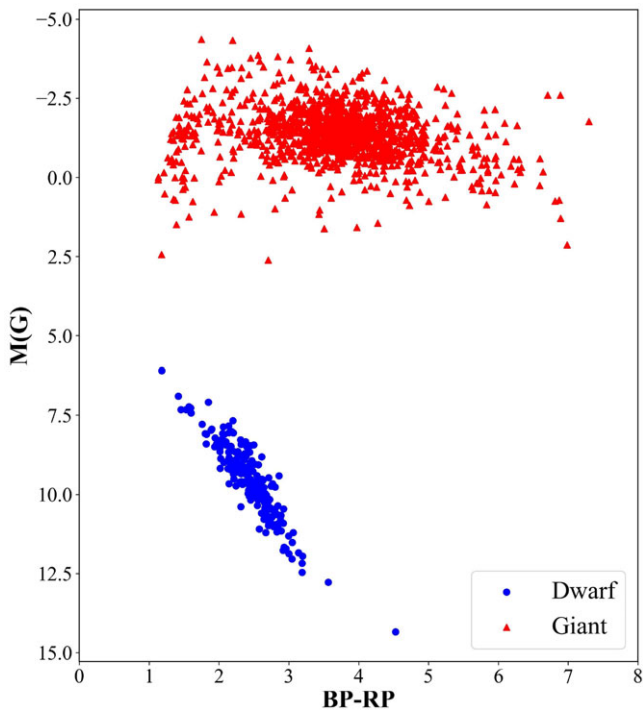


**Figure 6.** *Gaia* EDR3 absolute magnitude  $M(G)$  vs BP-RP colour for FBS M dwarfs (blue circles) and giants (M and N giants—red triangles) for comparison. The faintest object among the sample is M dwarf FBS 0250+167 ( $M(G) = 14.35$ ).

#### 4.7. The infrared emission. Spectral energy distribution (SED)

Infrared emission from M dwarfs has been investigated in multiple studies. Cotten & Song (2016) reported on about near 500 IR-excess stars. Extra flux in the IR range characterised the circumstellar dust which mark certain stages in the life of a planetary system (protoplanetary disc, and final stage is a debris disc, Luppe *et al.* (2020)). Sgro & Song (2021) used *Gaia* DR2 and ALLWISE W3 and W4 passbands to search for M dwarfs with IR-excess, within 100 pc. Using a special SED fitting algorithm, Sgro & Song (2021) developed a photospheric model for each sampled star, determined its significance of excess (SOE), and discussed the nature of IR excess in more detail.

We examine visually the SEDs for all FBS M dwarfs to search for possible dusty discs signature around them. All these SEDs have been built and taken from the SIMBAD VizieR database (access via <https://vizier.unistra.fr/vizier/sed/>) using the SED builder tool. Note that SEDs for objects presented in Tables 2, 3 and 4 apparently show plots for two objects, confirming the multiplicity these objects.

SEDs for a sample of 12 FBS M dwarfs (among the 236 dwarfs considered) with very clear IR-excess are shown in the panels of Figures 9–11. In SEDs of these objects, the excess IR radiation is clearly visible after 10  $\mu\text{m}$  (in WISE W3 and W4 passbands). An IR excess emission is not obvious in the SEDs of the other FBS M dwarfs.

In case of FBS 0909-082 (Figure 10), *Gaia* EDR3 and TESS data reveal two objects in 5 arcsec search. The existence of the secondary companion is well established in the SED of this object. Absolute similar SEDs show the objects *Gaia* DR2 2024760150182176896 and DR2 5480730048994706816, presented in paper by Sgro & Song (2021), with excess in IR emission.

An interesting line of future investigation would be to analyse the SEDs for all FBS M dwarfs using the spectral slope defined by Sgro & Song (2021) to measure the significance of excess (SOE).

## 5. Multiplicity. Possible companions

Multiplicity is the most common features of the stars in the Galaxy. About 35% of late-type main-sequence stars and 60% of known flare stars within 25 parsecs of the Sun are members of binary systems (Johnson *et al.* 1986). M dwarfs multiplicity rate has been investigated in many studies. For instance, stellar multiplicity among low-mass stars within 15 pc is presented by Ward-Duong *et al.* (2015). In many studies, authors typically explored the regions around M dwarfs in search of different types of objects at different separation from the star to identify substellar companions (small separation) and also wide binary systems (large separation). Finding and characterizing M dwarf multiples is useful in the study of transiting exoplanets, and multiplicity trends among them can yield insight into stellar formation and evolution (Lamman *et al.* 2020). Winters *et al.* (2019) have carried out the most comprehensive M dwarf multiplicity study, surveying volume-limited sample of 1120 dwarf primaries within 25 pc based on new observations, archived data, and literature search.

Currently, there are no direct and high-angular-resolution CCD imaging observations to search close companions around FBS newly detected M dwarfs. This type of observations is required to resolve the faint, close companions. As indicators for the possible presence of companions around FBS M dwarfs, we use high accuracy astrometric and photometric data mainly from the *Gaia* EDR3 and TESS catalogues. We also search for possible multiplicity data in the *Gaia* Catalogue of Nearby Stars (GCNS) database, for FBS M dwarfs up to 100 pc distances. Finally, as an additional indication, we check visually POSS II *I*-band direct images for FBS M dwarfs in STScI Digitized Sky Survey database [https://stdatu.stsci.edu/cgi-bin/dss\\_form](https://stdatu.stsci.edu/cgi-bin/dss_form).

### 5.1. *Gaia* EDR3 search

*Gaia* DR3 has the potential for extensive multiplicity studies. *Gaia* can resolve most companions down to 1 arcsec at magnitude contrast as large as six; closer systems are not resolved, regardless of secondary brightness (Ziegler *et al.* 2018; Lamman *et al.* 2020). Out of 176 of our cross-matched FBS new M dwarf targets, 27 have a second *Gaia* EDR3 object within the 5 arcsec search radius. In 19 cases out these 27, *Gaia* EDR3 database indicates a nearly equal magnitudes in *G*-band for companion. Three objects, FBS 0041+046, FBS 0820+035, and FBS 0828-087, are of particular interest. There are very close to primary M stars with an extremely faint second object in *G*-band (see detail below). The sensitivity of the *Gaia* data to closely separated binaries is expected to improve in future data releases.

### 5.2. TESS catalog search

TESS Input Catalog-v8.2 data indicate the presence of two objects in search radius 5 arcsec around position for 26 FBS M dwarfs. In 12 cases of out of these 26, the two objects have nearly-equal T (TESS T mag, Stassun *et al.* 2019) magnitudes. In this catalogue, three objects already pointed out above are rather exceptional with a bright primary star and very faint secondary companion.

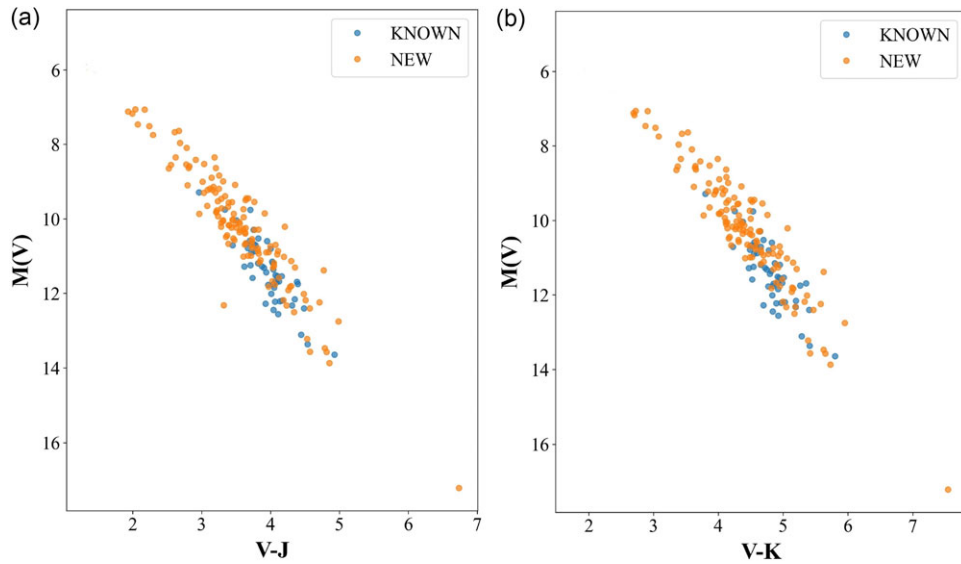


**Figure 7.** Observational HR diagram for FBS M dwarfs ( $M_V$  vs V-J and V-K colour based on TESS Input catalogue data with measured trigonometric parallaxes). Symbols are: orange dots-FBS M dwarfs (NEW), blue dots-M dwarfs KNOWN.

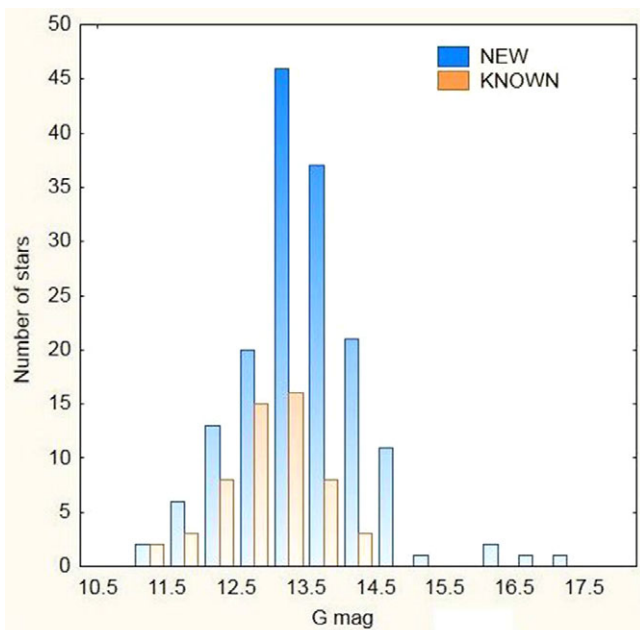


**Figure 8.** Histogram of the distribution of new FBS M dwarf sample (blue symbol) and known M dwarfs (orange symbol).

In Tables 2 and 3, consequently, *Gaia* EDR3 and TESS data are presented for these three FBS M dwarfs and their very close and faint companions.

There are no parallax information (positional data only) about the very faint and close objects around these three FBS M dwarfs in *Gaia* EDR3 and TESS databases. If these objects are gravitationally bound, i.e. they are physical companions at the same distances, their *G*-band absolute magnitudes can be determined:  $M(G) = 16.83, 17.37,$  and  $13.00$  for FBS 0041+046, FBS 0820+035, and for FBS 0828-087, respectively (Table 2). Such BP-RP colours and absolute *G*-band magnitudes place them on White Dwarfs

(WD) sequence on HRD (for detail see Figure 13 by Babusiaux et al. 2018).

Most probably, they are main-sequence M dwarf plus White Dwarf (dM + WD) binary systems. Note that these three FBS M dwarfs (Tables 2, 3) are also seen by GALEX satellite (Bianchi et al. 2017). For 9 FBS M dwarfs having GALEX associations, *Gaia* EDR3 data indicate 2 objects in the 5 arcsec search radius, but it is difficult to claim that the second companion is a WD because of the absence of the BP-RP colours. Based on Colour-Magnitude-Diagram (CMD), age dating analysis presented by Sgro & Song (2021) using BHAC15 isochrones, one can adopt a minimum age 0.1 Gyr for FBS 0041+046, 0.04 Gyr for FBS 0820+035, and 0.03 Gyr for FBS 0828-087 (see detail Chapter 4.1.1 and Figure 6 in Sgro & Song 2021).

### 5.3. *Gaia* Catalogue of Nearby Stars (GCNS) search

To search multiplicity and companions around new discovered FBS M dwarfs, we have cross-matched our results with the *Gaia* Catalogue of Nearby Stars (GCNS, *Gaia* Collaboration; Smart et al. 2019). To search multiplicity and companions around new discovered FBS M dwarfs, we have cross-matched with the *Gaia* Catalogue of Nearby Stars (GCNS, *Gaia* Collaboration; Smart et al. 2019). This catalogue has an estimated 331312 entries within 100 pc and gives information about 19176 resolved multiple systems.

Table 4 presents data for three FBS M dwarfs, which are presented as resolved binary systems in the GCNS database. Table 4 presents FBS Name for the bright, primary source (A), and for the secondary component (B), *Gaia* EDR3 source identifier, *Gaia* EDR3 *G*-band magnitude, BP-RP colour, *G*-band magnitude differences, angular separation of both objects, and projected separation in AU.

Figure 12 illustrates secondary physical components around three FBS M dwarfs on DSS2 I charts according to GCNS database.

For FBS 1107+350 GCNS gives 3 sources (*Gaia* Source ID 1 is 761700565771564416 and *Gaia* Source ID 2 is 761700462692366336) with angular separation 3.1798 arcsec, a

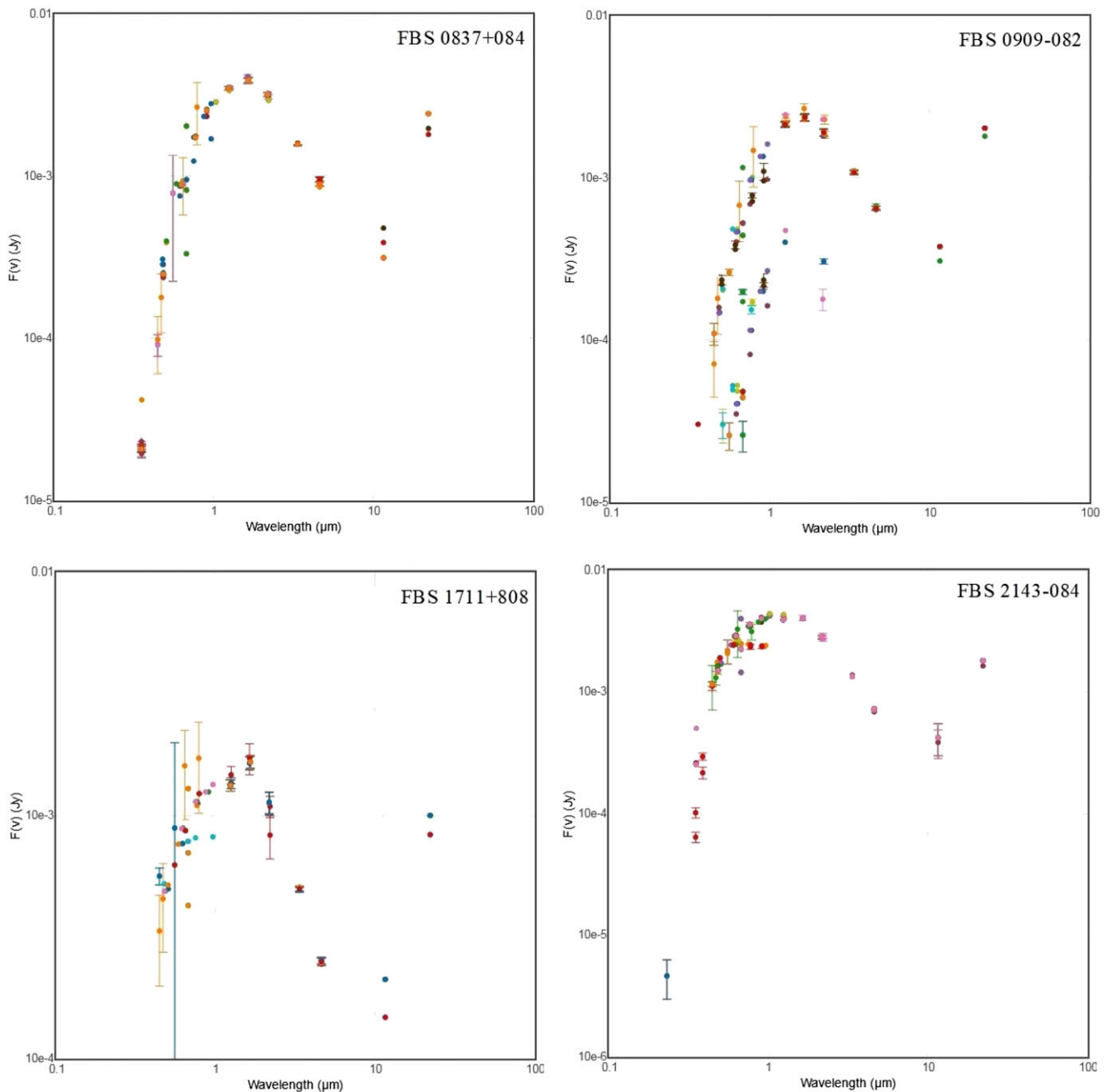


**Figure 9.** SEDs for four FBS M dwarfs built in Vizier data base using Gaia EDR3, POSSII-I, POSSII-I, POSSII-F, POSSII-J, Johnson-B, SDSS u, g, r, i, z, 2MASS J, H, Ks, WISE W1, W2, W3, and W4 photometric data (for more detail see <https://vizier.cds.unistra.fr/vizier/sed/>).

magnitude differences is 6.3433 mag, and projected separation is 190.6806 AU. Most probably, FBS 1107+350 is a triple system (Gaia third Source ID is 761700462692366336).

#### 5.4. Washington visual double star catalog

We also have cross-matched all FBS M dwarfs with the ‘Washington Visual Double Star Catalogue’ (WDS) objects (maintained by Brian Mason, 2001–2020, SIMBAD Vizier Catalog B/wds/wds; Mason *et al.* 2001) in order to find publications with information on multiple systems. Four objects out of 236, namely

FBS 0115-095, FBS 0913-103, FBS 1345+796, and FBS 1513+796, are associated with the visual double systems. Moreover, FBS 1345+796 is EA-type eclipsing binary.

As example, Figure 13 shows ASAS-SN (Shappee *et al.* 2014; Jayasinghe *et al.* 2018) light curve for M dwarf FBS 1345+796.

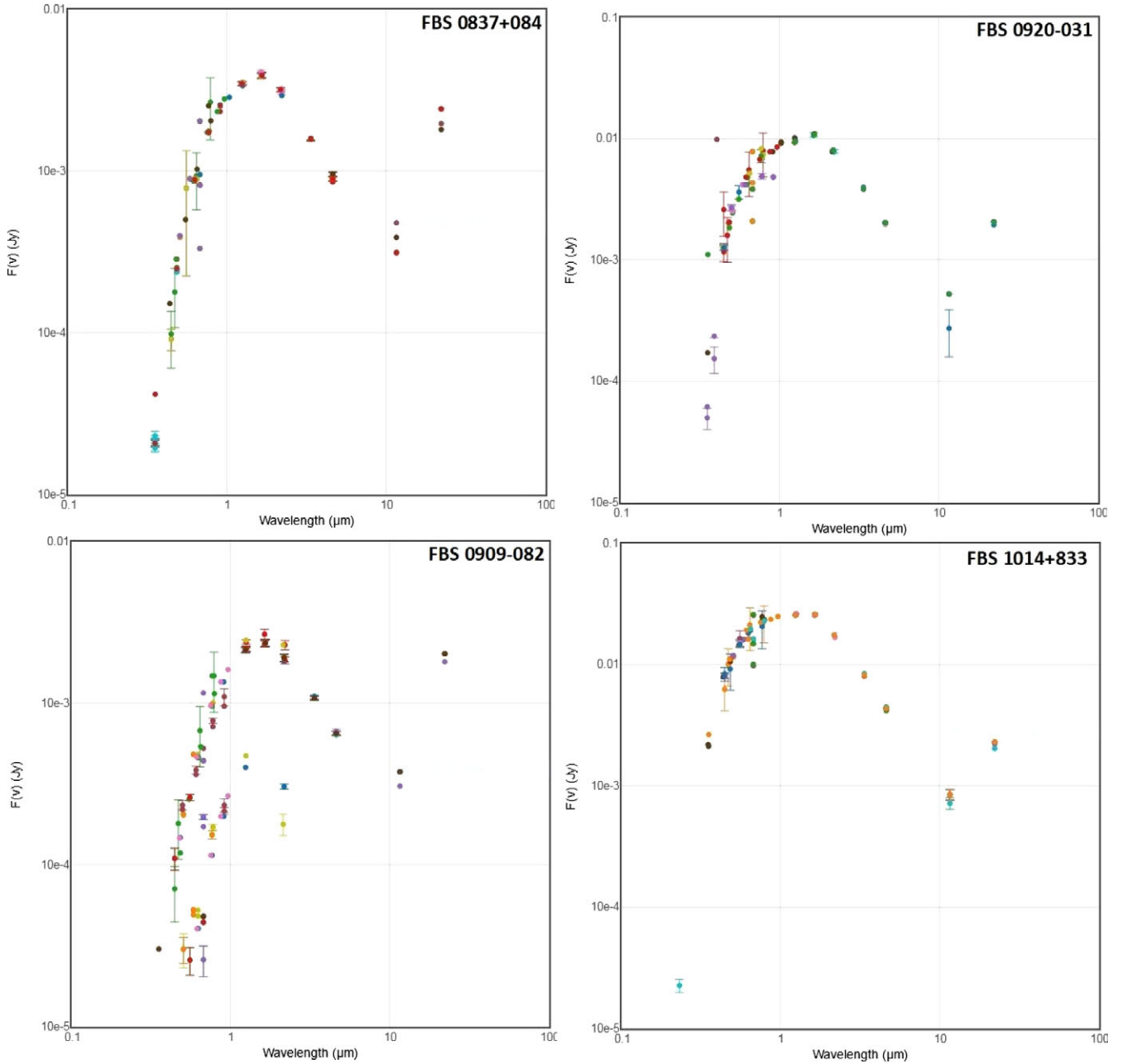
#### 5.5. Visual inspection of the POSS2 I images

With help of the data visualisation software SAOImage ds9, we search the POSS2 I-band images for possible companions



**Table 2.** Some important *Gaia* EDR3 catalogue data for three FBS M dwarfs.

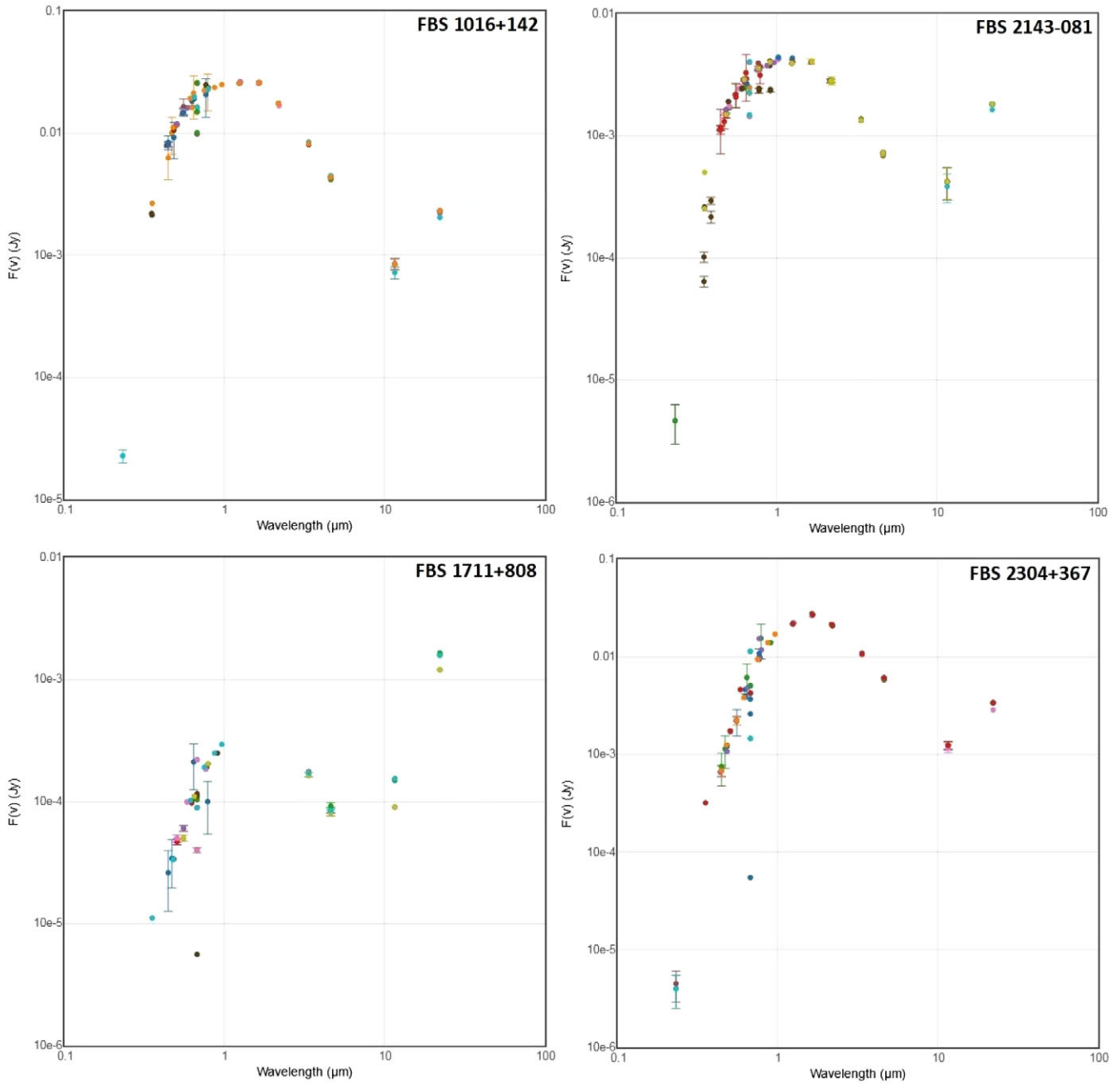
| FBS number | <i>Gaia</i> EDR3 number      | G mag | BP-RP mag | r (pc) | M(G)  |
|------------|------------------------------|-------|-----------|--------|-------|
| 0041+046   | (bright) 2554308108533636992 | 13.68 | 2.44      | 56.04  | 9.94  |
|            | (faint) 2554308108534379264  | 20.57 | 1.58      |        | 16.63 |
| 0820+035   | (bright) 3092033444148132224 | 13.48 | 2.68      | 49.23  | 10.00 |
|            | (faint) 3092030489210218240  | 20.83 | 1.66      |        | 17.37 |
| 0828-087   | (bright) 5752169164602798336 | 12.37 | 2.50      | 61.30  | 8.44  |
|            | (faint) 5752169160308040960  | 16.92 | 0.46      |        | 13.00 |



**Figure 10.** SEDs for four FBS M dwarfs built in Vizier data base using the same catalogue photometric data, as in Figure 9.

**Table 3.** Some important TESS catalog data for three FBS M dwarfs.

| FBS number | TESS input catalog identifier | TESS T mag | $T_{\text{eff}}$ K | Mass ( $M_{\odot}$ ) | Lumosity ( $L_{\odot}$ ) |
|------------|-------------------------------|------------|--------------------|----------------------|--------------------------|
| 0041+046   | (bright) 336565415            | 12.52      | 3464.0             | 0.366 (0.020)        | 0.01847(0.00448)         |
|            | (faint) 610931424             | 18.99      |                    |                      |                          |
| 0820+035   | (bright) 455236039            | 12.23      | 3340.0             | 0.386(0.020)         | 0.01751(0.00437)         |
|            | (faint) 804051355             | 19.76      |                    |                      |                          |
| 0828-087   | (bright) 51039965             | 11.18      | 3433.0             | 0.641(0.021)         | 0.05586(0.01311)         |
|            | (faint) 51039966              | 16.70      |                    |                      |                          |

**Figure 11.** SEDs for four FBS M dwarfs builded in Vizier database using the same catalogue photometric data, as in Figure 9.

**Table 4.** GCNS data for three new FBS M dwarfs as a binary systems.

| FBS number | <i>Gaia</i> EDR3 identifier | G mag. | G mag. diff | BP-RP colour | Angul. sep.(arcsec) | Proj. sep. (AU) |
|------------|-----------------------------|--------|-------------|--------------|---------------------|-----------------|
| 1009+350A  | 753259752444224000          | 14.28  | 2.62        | 2.41         | 3.431               | 249.95          |
| B          | 753259748150042752          | 16.91  |             | 3.08         |                     |                 |
| 1107+350A  | 761700565771564416          | 11.54  | 2.03        | 1.68         | 3.170               | 190.000         |
| B          | 761700565771564032          | 13.58  |             | 2.34         |                     |                 |
| 1136-082A  | 3591834837013732096         | 12.73  | 3.00        | 3.00         | 4.250               | 192.411         |
| B          | 3591834871372295040         | 15.74  |             | 2.69         |                     |                 |

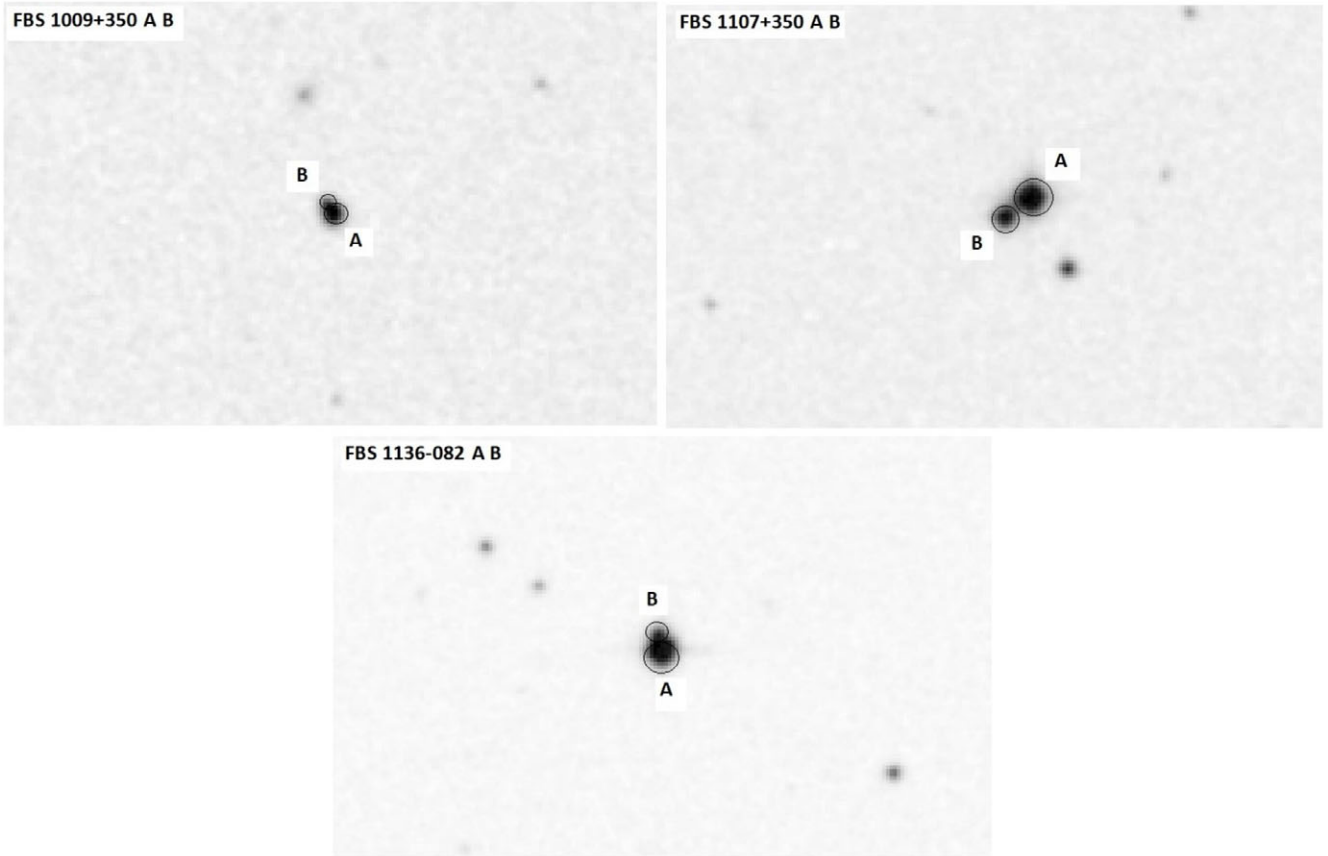


**Figure 12.** POSS2 I images for three FBS M dwarfs, which are included in GCNS catalogue as a binary systems. Physical components are circled and noted as B. They all are within 100 pc from the Sun. Very important note, the *Gaia* BP-RP colours for all components are typical for dwarf M stars. Field is 15 arcmin × 15 arcmin.

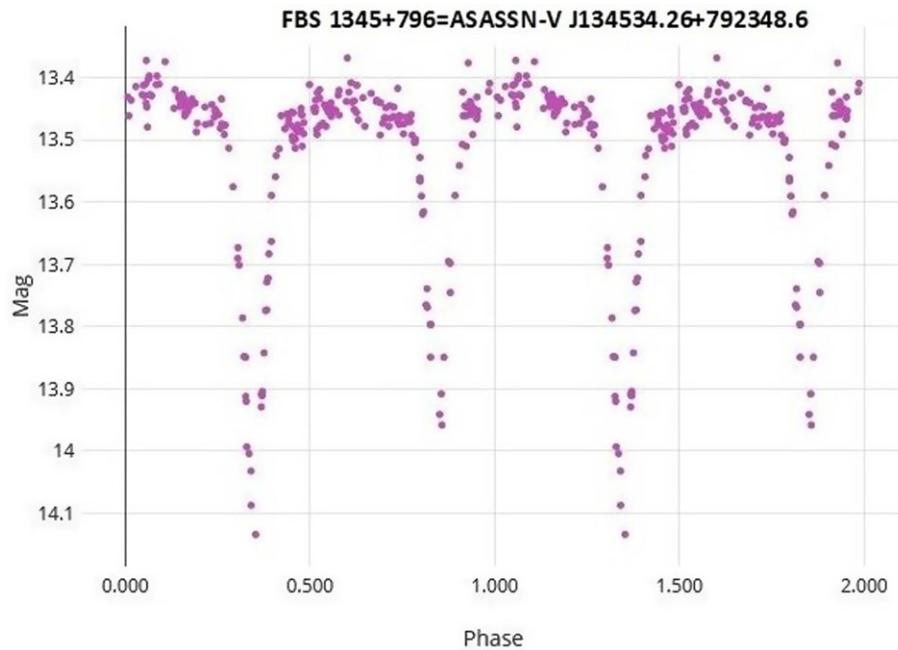
around the newly detected FBS M dwarfs. Such visualisation allows us to detect very close and comparatively bright possible physical companions around 6 dwarfs: FBS 0756+234, FBS 1010+205, FBS 1016+142, FBS 1340-049, FBS 1412-058, and FBS 1719+829. However, only in the case of FBS 0756+23,4 there is a very good match with the *Gaia* EDR3 catalogue distances (Bailer-Jones et al. 2021) for the primary M dwarf star and for very close companion. For the remaining 5 FBS M dwarfs, the distances for primary star and the faint close object are very different.

Figure 14 illustrates the POSS2 I-band image of the M dwarf star FBS 0756+234 and its companion. Spectra in the range

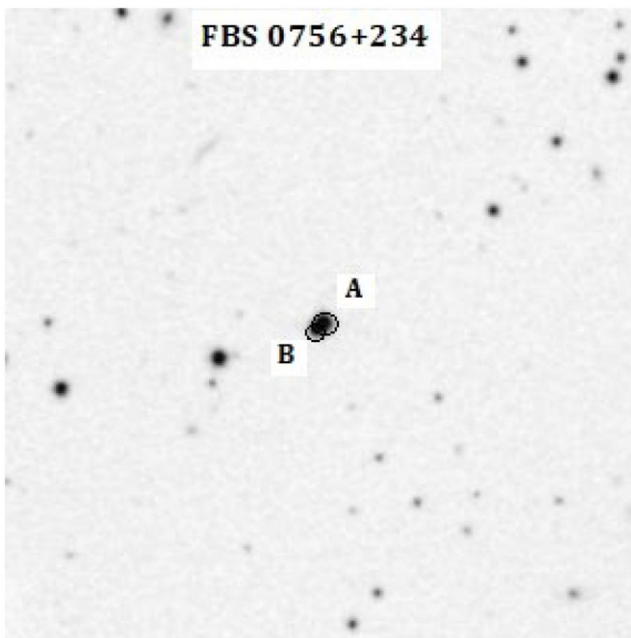
3900–9100 Å for this object was secured by LAMOST telescope and classified as dM4 type star (identifier is LAMOST J075935.66+232039.5, on-line access via <http://dr7.lamost.org/search/>).

Table 5 includes *Gaia* EDR3 and TESS data for dwarf M star FBS 0756+234 and for very close companion.

The BP-RP colour index and  $T_{eff}$  of the second and very close object are also typical for M dwarfs, therefore most probably, we have pair of M dwarfs (M dwarf + M dwarf). High-angular-resolution CCD is required to resolve very well the second component of FBS 0756+234 and faint companions around FBS M dwarfs in general.



**Figure 13.** ASAS-SN phased light curve for FBS 1345+796 classified as a EA-type eclipsing binary ( $P = 0.368$  d,  $\text{Ampl.} = 0.55$  mag,  $V_{\text{mean}} = 13.52$  mag) where the secondary eclipse is clearly seen.



**Figure 14.** POSS2 I image of dwarf M star FBS 0756+234 (primary star-A) and its closer companion (B) that we view as a binary system. Angular separation is  $1.74''$  arcsec on I-image. Field is  $5' \times 5'$ .

## 6. Analysis of TESS light curves of FBS M dwarfs

M dwarfs are favourable targets for transiting exoplanet surveys. TESS collected data for thousands of M dwarfs that might host habitable exoplanets. Detection of 1617 new transiting-planet candidates has been identified in the TESS full-frame images observed during the Primary Mission (Sectors 1–26; Kunimoto et al. 2022).

TESS data have been used in many studies devoted to detecting exoplanets around dwarf stars (Bryant & Bayliss 2022; Espinoza et al. 2022; Gilbert et al. 2022; Gan et al. 2022; Giacalone et al. 2022; Mori et al. 2022; Vach et al. 2022; Yee et al. 2022). We here apply the same methodology in the search of planets around FBS M dwarfs. We downloaded the Presearch Data Conditioning Simple Aperture Photometry (PDC-SAP) light curves from the Mikulski Archive for Space Telescopes (MAST—<https://mast.stsci.edu/portal/Mashup/Clients/Mast/Portal.html>). We then used lightkurve (<http://docs.lightkurve.org>) to download the target pixel files (TPFs) and to analyse light curves for FBS M dwarfs monitored by TESS. No transit events are detected when analysing TESS light curves.

TESS phase-dependent light curves show flares for many FBS M dwarfs. Figures 15 and 16 show examples of such flares in TESS light curves for objects FBS 0014-091 and FBS 0124-098. TESS light curve of FBS 0124-098 also shows very clear rotational modulation with period  $P = 3.51$  d (TIC Number is 299121712,  $M = 0.408 M_{\odot}$ ,  $L = 0.0231 L_{\odot}$ ,  $r = 53.81$  pc). The ROSAT association of this object is 1RXS J012724.3-093359. M dwarfs can be X-ray emitters if they have significant chromospheric activity with the best indicator of chromospheric magnetic activity being the  $H\alpha$  emission line (Yi et al. 2014). High activity levels are typically linked to rapid rotations, which in M dwarfs, is indicative of either spin-orbit coupling in close binary (Silvestri, Hawley, & Oswald 2005) or of young age (Silvestri et al. 2006). It is likely that FBS 0124-098 is a rapid rotator. We plan to investigate in detail magnetic activity and flare energies of DBS M dwarfs in the future.

## 7. Summary and future works

In order to gain more information on the M dwarfs identified in the First Byurakan Survey (FBS) low-resolution (lr) spectroscopic

**Table 5.** *Gaia* EDR3 and TESS catalogue data for dwarf M star FBS 0756+234.

| FBS number | <i>Gaia</i> EDR3 identifier | G mag | BP-RP colour | <i>Gaia</i> EDR3 distance(pc) | TIC number | Mass ( $M_{\odot}$ ) | Lum ( $L_{\odot}$ )       | TESS $T_{eff}$ (K) |
|------------|-----------------------------|-------|--------------|-------------------------------|------------|----------------------|---------------------------|--------------------|
| 0756+234A  | 680421917468548608          | 13.09 | 2.49         | 44.8166                       | 54233548   | 0.389( $\pm 0.021$ ) | 0.01992( $\pm 0.004888$ ) | 3437.0             |
| B          | 680421917468548480          | 14.58 | 2.82         | 44.7298                       | 54233549   | 0.224( $\pm 0.02$ )  | 0.00658( $\pm 0.00167$ )  | 3267.0             |

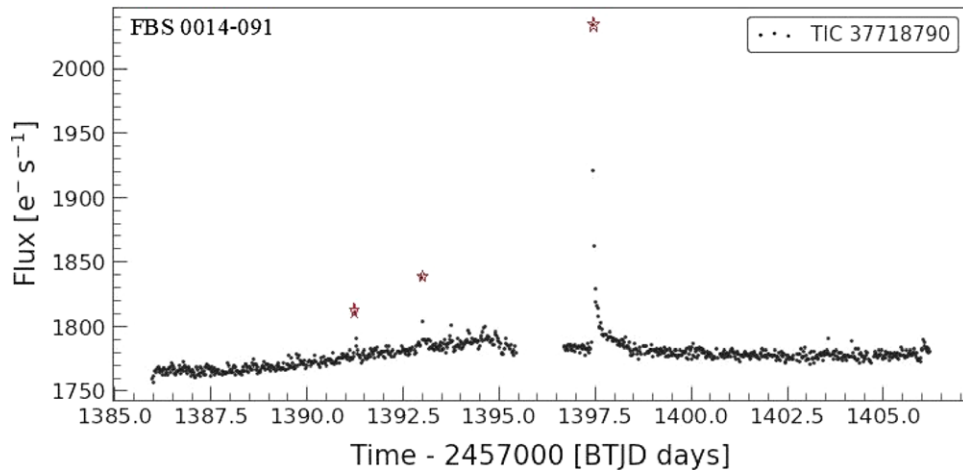


**Figure 15.** Demonstration of the detection of the TPF pipeline on example of the light curve for M dwarf FBS 0014-091 in TESS Presearch Conditioned Simple Aperture Photometry (PDC-SAP) from Sector 3. Red star symbols highlight the detection flare candidate peaks. The X-axis shows the time in Barycentric Julian Days (BJD), and Y-axis shows the normalised TESS PDC-SAP Flux.

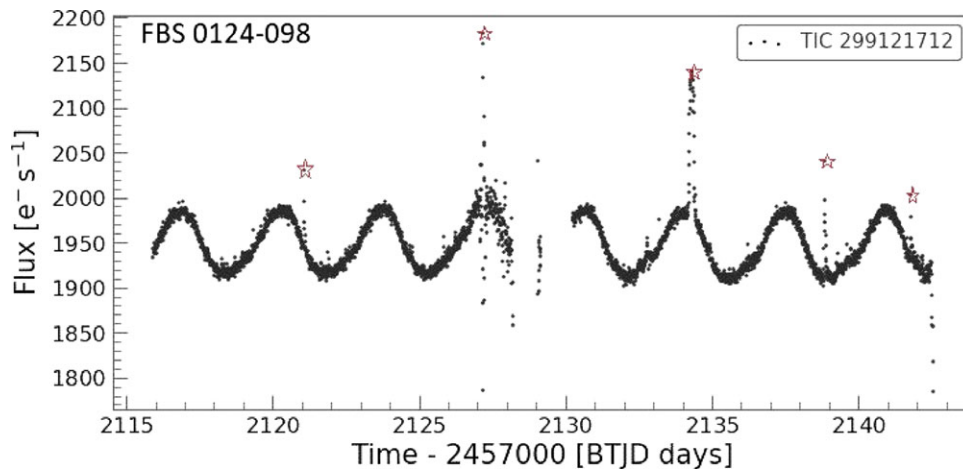


**Figure 16.** TESS light curve for M Dwarf FBS 0124-098 from Sector 30 reduced with help of pipeline TargetPixelFiles, where red star symbols highlight flare peaks. The X-axis shows the time in Barycentric Julian Days (BJD), and Y-axis shows the normalised TESS PDC-SAP Flux. The ROSAT association of this source is 1RXS J012724.3-093359.

database, *Gaia* EDR3 high-accuracy astrometric and photometric data and Transiting Exoplanet Survey Satellite (TESS) data are used to characterise these M dwarfs and their possible multiplicity. Among the sample 236 relatively bright M dwarfs, 176 are discoveries.

These objects are relatively bright with their 2MASS KS magnitude lying between 7.3 and 14.4. We also search visually POSS II I-images and cross-matched all M dwarfs with the *Gaia* Catalogue of Nearby Stars (GCNS) and with the Washington Visual Double

Star Catalogue. The *Gaia* EDR3 G broad-band magnitudes of the FBS M dwarfs are between  $11.3 < G < 17.1$ , their TESS estimated masses lie in the range  $0.095 (\pm 0.02) M_{\odot} \leq M \leq 0.7 (\pm 0.1) M_{\odot}$  and  $T_{eff}$  in the range  $4000 \text{ K} < T_{eff} < 2790 \text{ K}$ . We analyse various colour-colour diagrams of the new M dwarfs. For 27 FBS M dwarfs, *Gaia* DR3 and TESS catalogues indicate two objects within the 5 arcsec radius. Three out of these 27 objects, FBS 0041+046, FBS 0820+035, and FBS 0828-087, are most probably binaries with the companion being a White Dwarf (WD). Four objects

(FBS 0115-095, FBS 0913-103, FBS 1345+796, and FBS 1513+796) are found in the Washington Visual Double Star Catalogue. FBS 1345+796 is an EA-type eclipsing binary. According to Gaia EDR3 and TESS photometric data, FBS 0756+234 is most probably a close binary, and the *Gaia* EDR3 BP-RP colour diagrams for both objects are typical of M dwarfs. For FBS 1107+350, GCNS indicate 3 sources (*Gaia* Source ID 1 is 761700565771564416 and *Gaia* Source ID 2 is 761700462692366336) with angular separation 3.1798 arcsec, a difference in magnitude of 6.34 mag, and projected separation is 190.6806 AU. FBS 1107+350 represents most probably a triple system. If higher significance detection of the close companions around FBS M dwarfs are to be achieved and more knowledge about multiplicity of M dwarf be gained, high-angular-resolution CCD observations and possibly speckle interferometry are required for such studies.

Among the FBS sample considered, the FBS 0909-082 object is the most distant M dwarf ( $r = 780$  pc), with G-wide band absolute magnitude  $M(G) = 9.18$ ,  $M = 0.59 M_{\odot}$ ,  $L = 0.13597 L_{\odot}$ , and  $T_{\text{eff}} = 3844$  K. This object can be classified as M1-M2 subtype dwarf. The nearest object is FBS 0250+167, a M7 subtype dwarf with an extremely high proper motion ( $5.13$  arcsec  $\text{yr}^{-1}$ ), which is located at 3.83 pc from the Sun. As part of CARMENES search for exoplanets around M dwarfs, two exoplanets were found around this very high proper motion dwarf, each exoplanets with  $1.1 M_{\odot}$  minimum mass orbiting at periods of 4.91 and 11.4 d, respectively (Zechmeister et al. 2019). These two planets were among the lowest-mass planets discovered so far. We also analyse the TESS phase-dependent light curves from the Mikulski Archive for Space Telescopes (MAST) for the FBS dwarfs. TESS light curves do not show transit events. Nonetheless, TESS phase-dependent light curves indicate numerous flares of FBS M dwarfs.

Finally, for the first time, we estimate the detection limits of survey FBS for early and late-subclasses of M dwarfs with limiting magnitude 17.5–18.0 for FBS in  $V$ -band. Adopting  $M_V = 8.0$  for early-type M0 dwarfs (Reid et al. 2004), the detection range can be estimated at up to  $\sim 1000$  pc, and adopting  $M_V = 19.0$ – $20.0$  for M8-M9 dwarfs, the detection range can be estimated up to 25 pc for survey FBS.

This paper is the first report devoted to FBS M dwarfs with the presentation of some of their key physical parameters based on Gaia EDR3 and TESS data. Future work will be certainly on the study of flares and stellar activity, ages, and rotation rates of FBS M dwarfs.

**Acknowledgement.** This work was supported by ERASMUS+2019-1-FRO-KA107-061818. KSG and KKG are grateful to Administration of OVSQ Observatory and LATMOS Laboratory (France) for organizing their visit. This research has made use of results from the SAO/NASA Astrophysics Data System Bibliographic Services, as well as the SIMBAD and VizieR databases, operated at CDS, Strasbourg, France, and Two Micron All Sky Survey, which is a joint project of the University of Massachusetts and the Infrared Processing and Analysis Center, funded by NASA and NSF. This research was made possible using the ASAS-SN and Catalina Sky Survey variability data bases. We used LAMOST telescope spectra. The LAMOST is a National Major Scientific project build by the Chinese Academy of Sciences. This work has made use of data from the European Space Agency (ESA) mission *Gaia* (<https://cosmos.esa.int/gaia>), processed by Gaia Data Processing and Analysis Consortium (DPAC, <https://www.cosmos.esa.int/web/gaia.dpac.consortium>). This paper includes data collected by the TESS mission, which are publicly available from the Mikulski Archive for Space Telescopes (MAST). This research has made use of the Washington Double Star Catalog maintained at the US Naval Observatory.

We thank the anonymous referee for the thoughtful comments that greatly improved the clarity of the paper.

**Data availability.** Not applicable.

## References

- Abazajian, K. N., et al. 2009, *ApJS*, **182**, 543  
 Alonso-Floriano, F. J., et al. 2015, *A&A*, **577**, A128  
 Astudillo-Defru, N., et al. 2017, *A&A*, **602**, A88  
 Babusiaux, C., et al. 2018, *A&A*, **616**, A10  
 Bailer-Jones, C. A. L., Rybizki, J., Fousneau, M., Demleitner, M., & Andrae, R. 2021, *AJ*, **161**, 147  
 Baraffe, I., Homeier, D., Allard, F., & Chabrier, G. 2015, *A&A*, **577**, A42  
 Bessell, M. S. 1991, *AJ*, **101**, 662  
 Bessell, M. S., & Brett, J. M. 1988, *PASP*, **100**, 1134  
 Bianchi, L., Shiao, B., & Thilker, D. 2017, *ApJS*, **230**, 24  
 Boller, T., et al. 2016, *A&A*, **588**, A103  
 Brown, A. G. A., 2021, *A&A*, **650**, C3  
 Bryant, E. M., & Bayliss, D. 2022, *AJ*, **163**, 197  
 Cifuentes, C., et al. 2020, *A&A*, **642**, A115  
 Cotten, T. H., & Song, I. 2016, *ApJS*, **225**, 15  
 Cruz, K. L., et al. 2018, *AJ*, **155**, 34  
 Cui, X.-Q., et al. 2012, *RAA*, **12**, 1197  
 Delfosse, X., et al. 1999, *A&A*, **344**, 897  
 Delfosse, X., Forveille, T., Perrier, C., & Mayor, M. 1998, *A&A*, **331**, 581  
 Delfosse, X., et al. 2000, *A&A*, **364**, 217  
 Espinoza, N., et al. 2022, *AJ*, **163**, 133  
 Gan, T., et al. 2022, *MNRAS*, **511**, 83  
 Giacalone, S., et al. 2022, *AJ*, **163**, 99  
 Giclas, H. L., Burnham, R., & Thomas, N. G. 1971, Lowell proper motion survey Northern Hemisphere. The G numbered stars. 8991 stars fainter than magnitude 8 with motions  $> 0''.26/\text{year}$   
 Gigoyan, K., Mauron, N., Azzopardi, M., Muratorio, G., & Abrahamyan, H. V. 2001, *A&A*, **371**, 560  
 Gigoyan, K. S., et al. 2003, *Ap*, **46**, 475  
 Gigoyan, K. S., Mickaelian, A. M., & Kostandyan, G. R. 2019, *MNRAS*, **489**, 2030  
 Gilbert, E. A., et al. 2022, *AJ*, **163**, 147  
 Gliese, W., & Jahreiss, H. 1991, NASA STI/Recon Technical Report A, **224**, 161  
 Guerrero, N. M., et al. 2021, *ApJS*, **254**, 39  
 Henry, G. W., Fekel, F. C., Sowell, J. R., & Gearhart, J. S. 2006, *AJ*, **132**, 2489  
 Henry, J. P., et al. 1997, *AJ*, **114**, 1293  
 Henry, T. J., et al. 2018, *AJ*, **155**, 265  
 Jao, W.-C., et al. 2005, *AJ*, **129**, 1954  
 Jayasinghe, T., et al. 2018, *MNRAS*, **477**, 3145  
 Johnson, H. R., et al. 1986, The M-type stars  
 Kirkpatrick, J. D., et al. 1993, *ApJ*, **402**, 643  
 Kunimoto, M., et al. 2022, *ApJS*, **259**, 33  
 Lamman, C., et al. 2020, *AJ*, **159**, 139  
 Lépine, S., & Shara, M. M. 2005, *AJ*, **129**, 1483  
 Luo, A. L., et al. 2019, VizieR Online Data Catalog, V/164  
 Luppe, P., Krivov, A. V., Booth, M., & Lestrade, J.-F. 2020, *MNRAS*, **499**, 3932  
 Mann, A. W., et al. 2018, *AJ*, **155**, 4  
 Markarian, B. E., Lipovetsky, V. A., Stepanian, J. A., Erastova, L. K., & Shapovalova, A. I. 1989, *SoSAO*, **62**, 5  
 Martinez, A. O., et al. 2017, *ApJ*, **837**, 72  
 Mason, B. D., Wycoff, G. L., Hartkopf, W. I., Douglass, G. G., & Worley, C. E. 2001, *AJ*, **122**, 3466  
 Mori, M., et al. 2022, *AJ*, **163**, 298  
 Muirhead, P. S., et al. 2012, *ApJ*, **747**, 144  
 Paegert, M., et al. 2021, arXiv e-prints, [arXiv:2108.04778](https://arxiv.org/abs/2108.04778)  
 Pravdo, S. H., et al. 1999, *AJ*, **117**, 1616  
 Quirrenbach, A., et al. 2014, in Society of Photo-Optical Instrumentation Engineers (SPIE) Conference Series, Vol. 9147, Ground-based and Airborne Instrumentation for Astronomy V, ed. S. K. Ramsay, I. S. McLean, & H. Takami, 91471F

- Quirrenbach, A., et al. 2018, in Society of Photo-Optical Instrumentation Engineers (SPIE) Conference Series, Vol. 10702, Ground-based and Airborne Instrumentation for Astronomy VII, ed. C. J. Evans, L. Simard, & H. Takami, 107020W
- Reid, I. N., et al. 2004, *AJ*, **128**, 463
- Ricker, G. R., et al. 2014, in Society of Photo-Optical Instrumentation Engineers (SPIE) Conference Series, Vol. 9143, Space Telescopes and Instrumentation 2014: Optical, Infrared, and Millimeter Wave, ed. J. Oschmann, Jacobus M., M. Clampin, G. G. Fazio, & H. A. MacEwen, 914320
- Sgro, L. A., & Song, I. 2021, *MNRAS*, **508**, 3084
- Shappee, B. J., et al. 2014, *ApJ*, **788**, 48
- Silvestri, N. M., Hawley, S. L., & Oswald, T. D. 2005, *AJ*, **129**, 2428
- Silvestri, N. M., et al. 2006, *AJ*, **131**, 1674
- Skrutskie, M. F., et al. 2006, *AJ*, **131**, 1163
- Smart, R. L., et al. 2019, *MNRAS*, **485**, 4423
- Stassun, K. G., et al. 2018, *AJ*, **156**, 102
- Stassun, K. G., et al. 2019, *AJ*, **158**, 138
- Tarter, J. C., et al. 2007, *As*, **7**, 30
- Teegarden, B. J., et al. 2003, *ApJ*, **589**, L51
- Vach, S., et al. 2022, *AJ*, **164**, 71
- Voges, W., et al. 2000, *IAUC*, **7432**, 3
- Vrijmoet, E. H., et al. 2022, *AJ*, **163**, 178
- Ward-Duong, K., et al. 2015, *MNRAS*, **449**, 2618
- West, A. A., et al. 2011, *AJ*, **141**, 97
- Winters, J. G., et al. 2019, *AJ*, **157**, 216
- Yee, S. W., et al. 2022, *AJ*, **164**, 70
- Yi, Z., et al. 2014, *AJ*, **147**, 33
- Zechmeister, M., et al. 2019, *A&A*, **627**, A49
- Zhong, J., et al. 2019, *ApJS*, **244**, 8
- Ziegler, C., et al. 2018, *AJ*, **156**, 259